



## MECHANICAL AND ELECTRICAL PROPERTIES OF THE TERNARY CU-GE-PB AND CU-GE-IN ALLOYS

*Milan Milosavljević<sup>57</sup>; Aleksandar Djordjević<sup>58</sup>; Duško Minić<sup>59</sup>;  
Milena Premović Zečević<sup>60</sup>; Milan Kolarević<sup>61</sup>*

### Abstract

This study presents the results of experimental and analytical testing of the microstructure, hardness and electrical properties of selected triple Cu-Ge-Pb and Cu-Ge-In systems. In the experimental part of the paper, alloys of selected compositions were prepared which were then examined by scanning electron microscopy (SEM) and energy dispersive spectrometry (EDS), X-ray powder diffraction (XRD), Brinell hardness measurements and electrical conductivity measurements. The phase diagram of equilibrium ternary systems was calculated using the Calphad method and the corresponding thermodynamic program Pandat ver. 8.1. The results include the calculated characteristic isothermal sections, structural characteristics, phase composition, mechanical properties and electrical conductivity for ternary Cu-Ge-Pb and Cu-Ge-In systems. Isothermal sections at 25 °C were extrapolated using optimized thermodynamic parameters from the literature. The experimentally obtained results were compared with the results of thermodynamic calculation of phase diagrams. A good general agreement was obtained between the experimental and calculated values. The hardness and electrical conductivity of the selected alloys were measured and using the appropriate mathematical model, these properties were predicted in the entire range of the composition.

*Key words: Cu-Ge-Pb system, Cu-Ge-In system, experimental test, isothermal sections, hardness measurement, electrical conductivity measurement.*

---

<sup>57</sup>Milan Milosavljevic, Ph.D., University of Priština, Faculty of Technical Science, Kos. Mitrovica, Republic of Serbia, milan.milosavljevicm@gmail.com

<sup>58</sup>Aleksandar Djordjević Assistant Professor, PhD, Academician of IRASA, University of Priština, Faculty of Technical Science, Kos. Mitrovica, Republic of Serbia, coadjordjevic90@gmail.com

<sup>59</sup>Duško Minić, Full Professor, PhD, Academician of IRASA, University of Priština, Faculty of Technical Science, Kos. Mitrovica, Republic of Serbia, dminic65@mts.rs

<sup>60</sup>Milena Premović Zečević, Associate Professor, PhD, Academician of IRASA, University of Priština, Faculty of Technical Science, Kos. Mitrovica, Republic of Serbia, milena.premovic@gmail.com

<sup>61</sup>Milan Kolarevic, Full Profesor, PhD, University of Kragujevac, Faculty of Mechanical Engineering in Kraljevo, Republic of Serbia, kolarevic.m@mfkv.kg.ac.rs



## Introduction

The ternary Cu-Ge-In and Cu-Ge-Pb systems has been previously investigated by our group [1, 2]. In the ternary Cu-Ge-In system, three vertical sections (Cu-GeIn, Ge-CuIn and In-CuGe) and two isothermal sections at 200 and 300 °C were tested [1]. For the ternary Cu-Ge-Pb system, three vertical section (Cu-GePb, Ge-CuPb and Pb-GeCu) and two isothermal sections at 600 and 400 °C were tested [2]. In this paper, microstructure, mechanical and electrical properties have been tested. Selected systems are due to their good thermal and electrical conductivity and strength [3-6]. Systems containing some of these elements have also been previously examined [7-10]. In this paper, the focus is given to systems based on copper [11-13] and germanium [14-16], which are of great interest nowadays. In addition to mechanical and electrical properties, an isothermal section at 25 °C was also tested. Used experimental techniques were scanning electron microscopy (SEM) with energy dispersive spectroscopy (EDS), X-ray diffractometric analysis (XRD), light optical microscopy (LOM), hardness and electrical conductivity test. Experimental results of the EDS and XRD tests were compared with calculated phase diagram of isothermal section at 25 °C and a good agreement has been reached. By using experimental results of the hardness and electrical conductivity and an appropriate mathematical model, those properties were predicted along all composition range.

## Experimental procedure

Twelve ternary samples per ternary systems were prepared. Prepared samples were from high purity elements (Cu, Ge, In and Pb). Total mass of each sample were 3gr. After weighting of samples, samples were melted in an arc furnace under high-purity argon atmosphere and slowly cooled to the room temperature. The average weight loss during melting was about 0.5 mass %. Such prepared samples are subjected to all experimental tests.

## Results and Discussions

The same experimental techniques were applied to each ternary sample. Firstly, XRD test were performed to determined phases presented in microstructure. Composition of samples and composition of presented phases inside samples were examined with EDS test. EDS test confirmed predicted phases by XRD test. The EDS composition of samples were mapped on calculated isothermal section at 25 °C. Experimentally determined phases by EDS and XRD were compared with predicted phases of calculated isothermal section at 25 °C. LOM were used for presentation of observed microstructures. After LOM electrical conductivity tests were performed on four different point. The last test was the measurement of hardness. Hardness test were measured on three different point. Experimentally determined electrical conductivity



and hardness results were used for modeling of those properties along all composition ranges.

### Ternary Cu-Ge-In system

According to the results of Milosavljevic et al. [1], in the ternary Cu-Ge-In system thirteen solid phases can appear. According to the previous work in the ternary system there is no ternary compound, large solubility of the third element in phases  $\xi$ ,  $\varepsilon$ ,  $\eta$ ,  $\theta$ ,  $\beta$ ,  $\gamma$ ,  $\delta$ ,  $\eta'$ ,  $\eta''$  and  $\text{Cu}_{11}\text{In}_9$  as well in (Cu), (Ge) and (In) solutions.

### Microstructural analysis

According to the XRD and EDS results on 12 samples, four different phase regions were determined. Samples 1, 5-8, and 10-12, have three phases in microstructure (Ge)+(In)+ $\text{Cu}_{11}\text{In}_9$ . Sample 2 have three phases  $\eta''$ , (Ge) and  $\text{Cu}_{11}\text{In}_9$ . Samples 3 and 9 determined same three phase region  $\eta+\eta''$ +(Ge). Sample 4 have three phases  $\delta+\xi+\eta$ . Phases determined by XDR are confirmed by EDS. Calculated isothermal section is given on Figure 1.

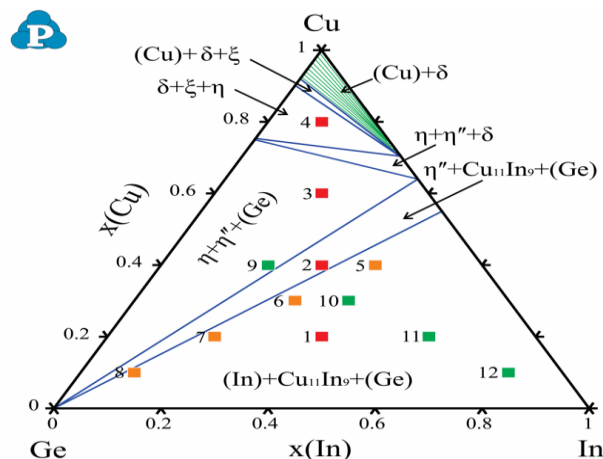


Figure 1. The predicted isothermal section at 25 °C and composition of 12 ternary samples.

Calculated isothermal section consist of six three phase regions and six two phase regions. Two phase regions such as  $\text{Cu}_{11}\text{In}_9$ +(Ge),  $\eta''$ +(Ge),  $\eta+\eta''$ ,  $\eta+\delta$  and  $\delta+\xi$  are settled on line which divides closes three phase regions. Experimental results confirmed four three phase regions. Microstructure of 12 ternary samples were recorded by LOM. Figure 2, presents three microstructure of samples 2, 3 and 6 as one illustration.

Selected LOM microstructures of samples 2, 3 and 6 have three phases in microstructures. In each microstructure (Ge) phase appears as a gray phase. Beside (Ge) phase in sample 2  $\text{Cu}_{11}\text{In}_9$  and  $\eta''$  have been detected.  $\text{Cu}_{11}\text{In}_9$  phase appears as a light needle phase while  $\eta''$  phase is light gray phase. In microstructure 3, (Ge) is a gray phase,  $\eta''$  is a light gray phase and  $\eta$  is a oval phase. In microstructure of sample

6, (Ge) is a gray phase, (In) as a light gray phase and  $\text{Cu}_{11}\text{In}_9$  phase as a light needle phase.

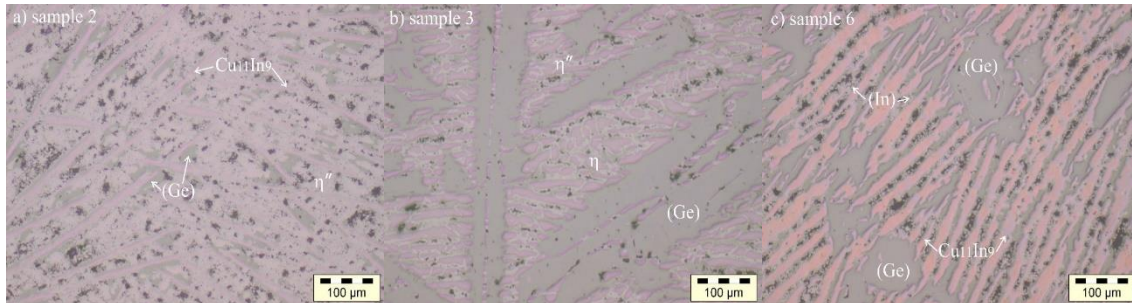


Figure 2. LOM micrographs of samples a) 2, b) 3 and c) 6.

### Mechanical properties

Mean value of Brinell hardness depending of alloys composition are graphically presented on Figure 3.

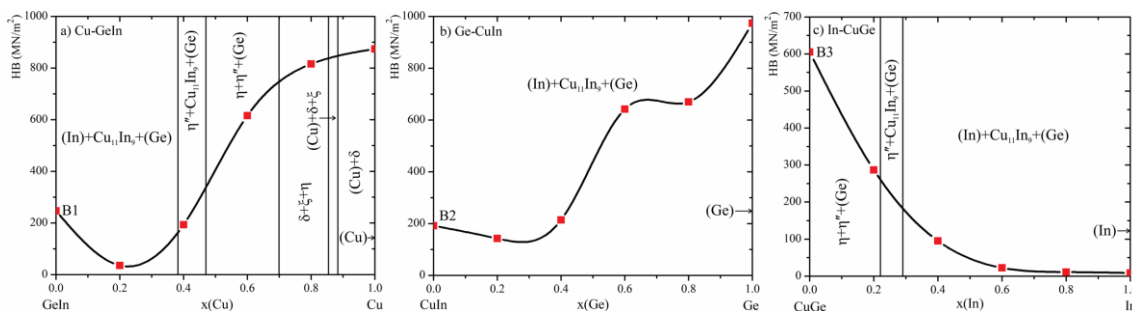


Figure 3. Graphical presentation of Brinell hardness dependence of composition: a) vertical section Cu-GeIn, b) vertical section Ge-CuIn and c) vertical section In-CuGe

Microstructure strongly influence on alloys properties. In addition to the microstructure, the percentage of the phase also plays an important role. For example in samples 1, 5-8, and 10-12, same microstructure  $(\text{Ge})+(\text{In})+\text{Cu}_{11}\text{In}_9$  is presented but hardness significantly change. From all ternary samples where three phase region  $(\text{Ge})+(\text{In})+\text{Cu}_{11}\text{In}_9$  is detected the highest hardness have sample 8, 670.03  $\text{MN}/\text{m}^2$ . Sample 8, consist of 80% of (Ge) solid solution, 1.82% (In) solid solution and 18.18%  $\text{Cu}_{11}\text{In}_9$  intermetallic compound. So, it is clear that percent of (Ge) solid phase is responsible for high hardness. From all tested ternary samples, the highest hardness has been detected on sample 4. Detected hardness is 815.53  $\text{MN}/\text{m}^2$ . Result of such a high hardness belongs to the intermetallic compounds and their crystal structure. By utilizing experimentally determined values of hardness mathematical model of the dependence of the Brinell hardness on composition for the Cu-Ge-In alloys was developed. It is proposed „Quadratic Mixture model“.

The final equation of the predictive model in terms of real components is (1):  

$$\text{HB}(\text{MN}/\text{m}^2) = 988.57589 \cdot (\text{Cu}) + 1005.59551 \cdot (\text{Ge}) + 4.70156 \cdot (\text{In}) - 1385.51524 \cdot (\text{Cu}) \cdot (\text{Ge})$$



$$-1250.33062*(Cu)*(In)-1326.08583*(Ge)*(In) \quad (1)$$

Iso-lines contour plot for Brinell hardness of alloys defined by equation (1) is shown in Figure 4.

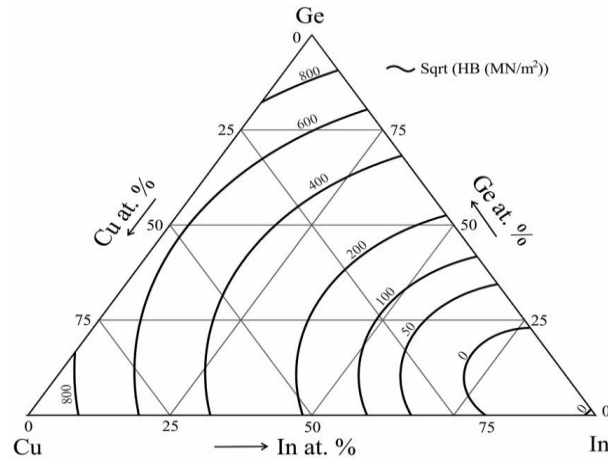


Figure 4. Calculated iso-lines of Brinell hardness in ternary Cu-Ge-In system with  $R^2 = 0.908$ .

### Electrical properties

For better presentation of results, Figure 5 has been plotted. Presented is relationship between the electrical conductivity of the tested alloys and the composition of the alloys.

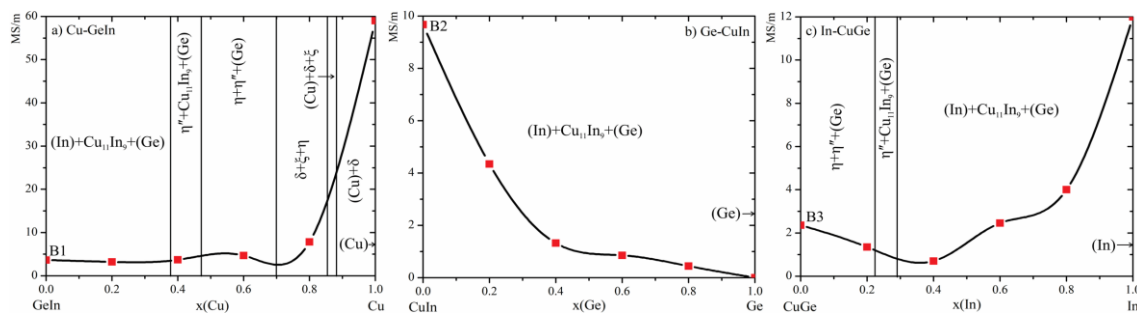


Figure 5. Graphical presentation of electrical conductivity dependence of composition and phase fraction a) vertical section Cu-GeIn, b) vertical section Ge-CuIn and c) vertical section In-CuGe.

According to the obtained results it is clear that sample 4, have best electrical conductivity in comparison with other testes ternary samples. Good electrical conductivity is related to the microstructure of samples. In sample 4, dominant phase is  $\xi$  with 44 %, then  $\delta$  phase with 33.33 % and  $\eta$  phase with 22.67 %. Beside microstructure high value of electrical conductivity is linked with high amount of copper in sample 4.

By using experimental data of electrical conductivity the same methodology was applied in the process of obtaining models for electrical conductivity. „Quadratic





Mixture model" was suggested as a final equation for prediction of electrical conductivity.

The final equation of the predictive model in terms of actual components is:

$$\begin{aligned} \ln(EP+3.00) = & 3.930479473*(Cu)+1.155188289*(Ge)+2.549564358*(In) \\ & -4.233555034*(Cu)*(Ge)-4.03567672*(Cu)*(In) \end{aligned} \quad (2)$$

Iso-lines contour plot for electrical conductivity of Cu-Ge-In alloys defined by equation (2) is shown in Figure 6.

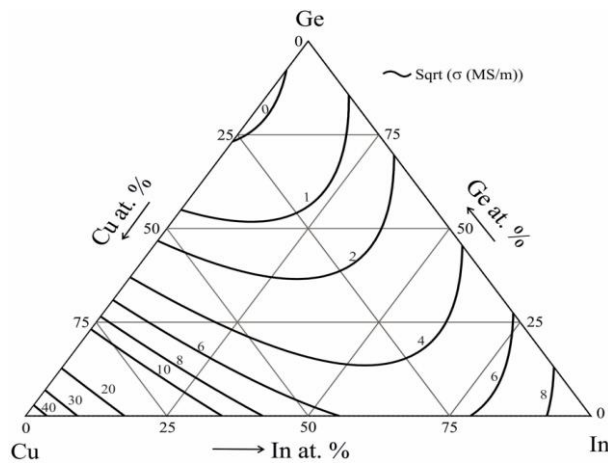


Figure 6. Calculated iso-lines of electrical conductivity in ternary Cu-Ge-In system with  $R^2 = 0.907$ .

### Ternary Cu-Ge-Pb system

#### Microstructural analysis

Figure 7 presents calculated isothermal section at 25 °C for a ternary Cu-Ge-Pb system. On Figure 7 were marked and nominal composition of samples.

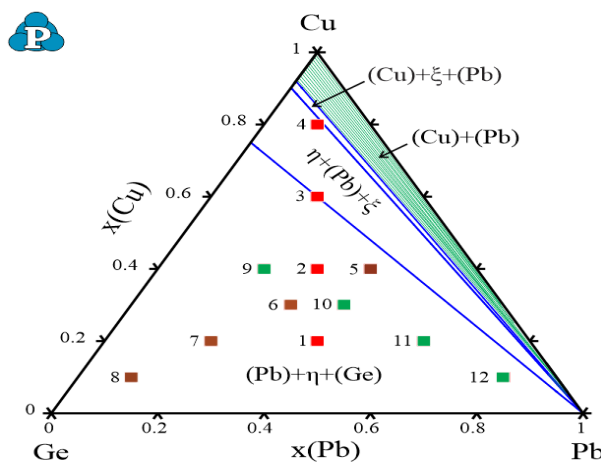


Figure 7. The predicted isothermal section at 25 °C and composition of 12 ternary samples

Four phase regions are visible on the calculated isothermal section at 25 °C. One region is two-phase region and three are three-phase regions. From the four calculated phase regions, the existence of two have been experimentally confirmed. The confirmed phase regions are: (Pb)+η+(Ge) with samples 1,2 and 5-12, and η+(Pb)+ξ, with samples 3 and 4. It is clear that the experimentally determined phase compositions are very close to the calculated phase compositions. From this it can be concluded that the experiments support the calculated isothermal section at 25 °C quite well.

Figure 8, presents three microstructure of samples 6 and 4 as one illustration.

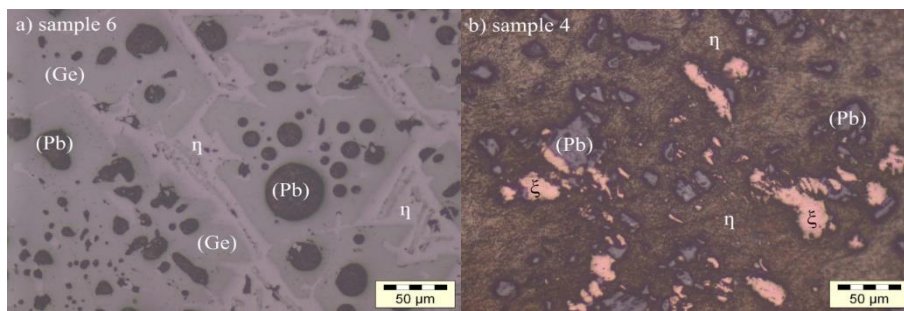


Figure 8. LOM micrographs of a) sample 6 and b) sample 4.

Selected LOM microstructures of samples 6 and 4 have three phases in microstructures. In microstructure of the sample 6, (Ge) is a gray phase, η is a light gray phase and (Pb) is a dark phase. In microstructure of sample 4, (Pb) is a gray phase, η is a dark gray phase and ξ phase is a light phase.

### *Mechanical properties*

Mean value of Brinell hardness depending of alloys composition are graphically presented on Figure 9.

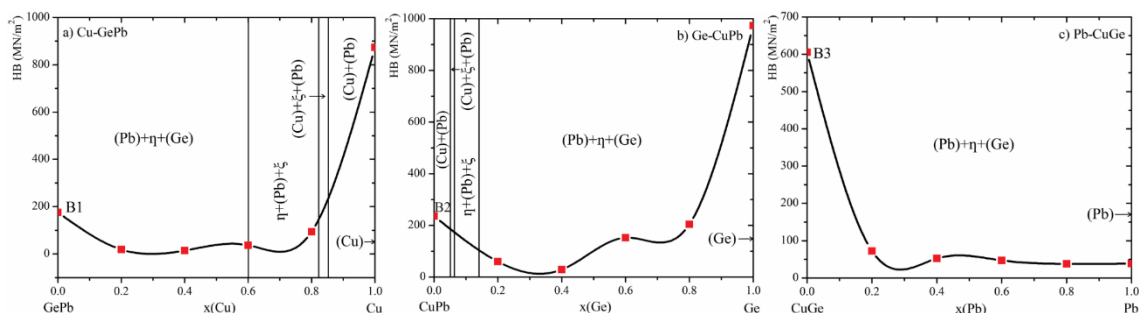


Figure 9. Graphical presentation of Brinell hardness dependence of composition and phase fraction: a) vertical section Cu-GePb, b) vertical section Ge-CuPb and c) vertical section Pb-CuGe.

Based on the obtained results graphically shown in Figure 9, it can be seen that the highest value of hardness was recorded on sample 8. The lowest Brinell hardness value was recorded on sample 2. Figure 9a) shows the hardness of alloys by increasing the copper content. As the copper content of the alloys increases, the hardness of the



## SETI IV 2022

Book of Proceedings

alloy constantly increases. Figure 9b) shows the hardness behavior of alloys by increasing the germanium content. Experimental results show that the addition of germanium increases the hardness. Figure 9c) shows the hardness of alloys with increasing lead content and the results show that the addition of lead reduces the hardness of alloys.

By utilizing experimentally determined values of hardness, mathematical model of the dependence of the Brinell hardness on composition for the Cu-Ge-Pb alloys was developed.

The final equation of the predictive model in terms of real components is:

$$\ln(\text{HB}) = 6.163185018x(\text{Cu}) + 6.79963598x(\text{Ge}) + 3.708216051x(\text{Pb}) - 1.805993x(\text{Cu})x(\text{Ge}) + 1.302482727x(\text{Cu})x(\text{Pb}) - 0.18806291x(\text{Ge})x(\text{Pb}) - 58.1002277x(\text{Cu})x(\text{Ge})x(\text{Pb}) \quad (3)$$

Iso-lines contour plot for Brinell hardness of alloys defined by equation (3) is shown in Figure 10.

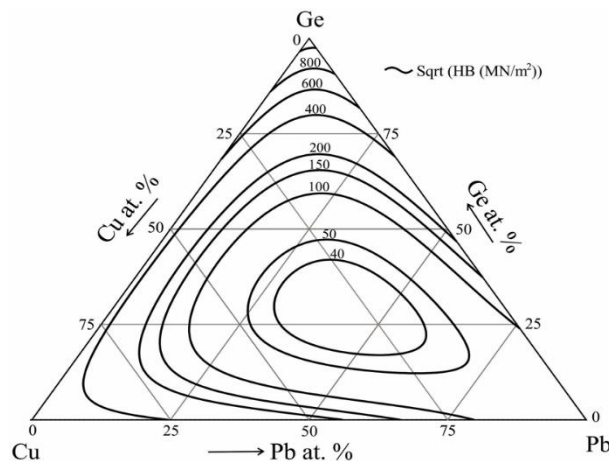


Figure 10. Calculated iso-lines of Brinell hardness in ternary Cu-Ge-Pb system with  $R^2 = 0.83$ .

### *Electrical properties*

For better presentation of results, Figure 11 has been plotted. Presented is relationship between the electrical conductivity of the tested alloys and the composition of the alloys.

Good electrical conductivity is related to the microstructure of samples. Beside microstructure high value of electrical conductivity is linked with high amount of one of the elements in sample.

The mathematical model was transformed using the „Natural Log“ function. ANOVA analysis confirmed the adequacy of the transformed model.



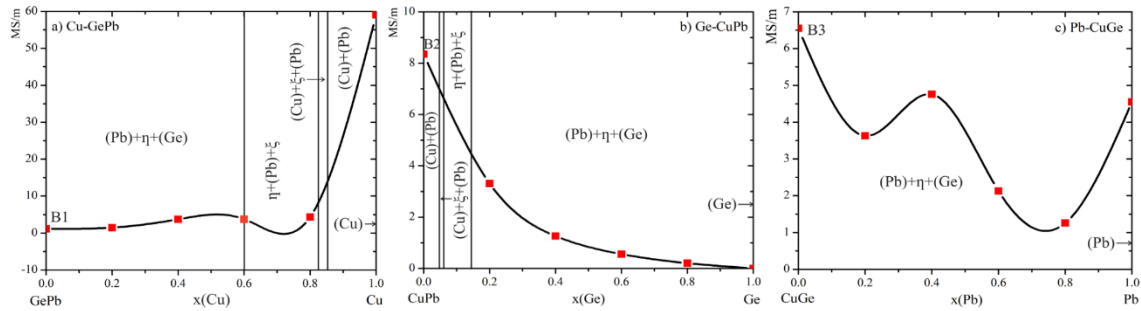


Figure 11. Graphical presentation of electrical conductivity dependence of composition and phase fraction a) vertical section Cu-GePb, b) vertical section Ge-CuPb and c) vertical section Pb-CuGe.

The final equation of the predictive model in terms of actual components is:  
$$\ln(EP + 0.01) = 3.679702885x(\text{Cu}) - 2.797254784x(\text{Ge}) + 1.278833776x(\text{Pb}) \quad (4)$$

Iso-lines contour plot for electrical conductivity of Cu-Ge-Pb alloys defined by equation (5) is shown in Figure 12.

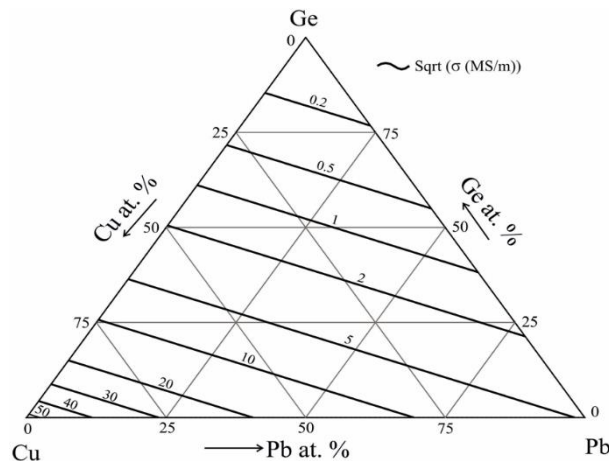


Figure 12. Calculated iso-lines of electrical conductivity in ternary Cu-Ge-Pb system with  $R^2 = 0.81$ .

## Conclusions

In this paper, twelve ternary alloys from Cu-Ge-In system and twelve ternary alloys from Cu-Ge-Pb system were investigated. Alloys were tested experimentally by using SEM-EDS, XRD, LOM, hardness tests and electrical conductivity tests. Beside experimental test, isothermal sections at 25 ° C were calculated by using Pandat software. The phase regions in the calculated isothermal section were experimentally determined by the XRD and EDS analysis and good agreement was reached between the results of the calculation and the experiments. Hardness by Brinell and electrical conductivity were tested and experimental results were used for development of



appropriate mathematical model. Mathematical model was used for predicting those properties along all composition ranges.

## References

- [1] Milosavljevic, M. Premovic, M., Minic, D., Manasijevic, D., Djordjevic, A., Tomovic, M. Thermodynamic Description of the Cu-Ge-In System: Experiment and modeling, *JPED.*, (2021), 42, pp. 851-863.
- [2] M. Milosavljevic, M. Premovic, D. Minic, D. Manasijevic, A. Todic, M. Tomovic, Thermodynamic description of the Cu-Ge-Pb system: Experiment and modeling, *Calphad*, (2021), 72, pp. 102216.
- [3] H. Kim, J. H. Ahn, S. Z. Han, J. Jo, H. Baik, M. Kim, H. N. Han, Microstructural characterization of cold-drawn CuNiSi alloy having high strength and high conductivity, *J. of All. and Comp.*, (2020), 832, pp. 155059.
- [4] Y. Cao, S. Z. Han, E. A. Choi, J. H. Ahn, X. Mi, S. Lee, H. Shin, S. Kim, J. Lee, Effect of inclusion on strength and conductivity of Cu-Ni-Si alloys with discontinuous precipitation, *J. of All. and Comp.*, (2020), 843, pp. 156006.
- [5] J. Li, G. Huang, X. Mi, L. Peng, H. Xie, Y. Kang, Microstructure evolution and properties of a quaternary Cu-Ni-Co-Si alloy with high strength and conductivity, *Mat. Science and Engin.: A*, (2019), 766, pp. 138390.
- [6] V. P. Vassiliev, V. A. Lysenko, Thermodynamic assessment of the Cu-In-Pb system, *J. of All. and Comp.*, (2015), 629, pp. 326-331.
- [7] V. P. Vassiliev, V. A. Lysenko, W. P. Gong, New EMF measurements and thermodynamic evaluation of the In-Pb-Zn system, *J. of All. and Comp.*, (2013), 564, pp. 49-54.
- [8] S. Jin, L. I. Duarte, C. Leinenbach, Experimental study and thermodynamic description of the Au-Cu-Ge system, *J. of All. and Comp.*, (2014), 588, pp. 7-16.
- [9] J. Wang, Y. J. Liu, C. Y. Tang, L. B. Liu, H. Y. Zhou, Z. P. Jin, Thermodynamic description of the Au-Ag-Ge ternary system, *Therm. Acta*, (2011), 512(1-2), pp. 240-246.
- [10] D. Orac, M. Laubertova, J. Piroskova, D. Klein, R. Bures, J. Klimko, Characterization of dusts from secondary copper production, *JMM, Section B: Metallurgy*, (2020), 56(2) B, pp. 221-228.
- [11] B. Dong, X. Cai, S. Lin, X. Li, C. Fan, C. Yang, H. Sun, Wire arc additive manufacturing of Al-Zn-Mg-Cu alloy: Microstructures and mechanical properties, *Add. Man.*, (2020), 36 pp. 101447.
- [12] A. Kamegawa, T. Kuriwa, M. Okada, Effects of dehydrogenation heat-treatment on electrical-mechanical properties for hydrogenated Cu-3 mass%Ti alloys *J. of All. and Comp.*, (2013), 566, pp. 1-4.
- [13] S. Adachi, *Properties of Semiconductor Alloys: Group-IV, III-V and II-VI, Semiconductors*, Wiley, Hoboken, (2009).
- [14] A. Rockett, *The Materials Science of Semiconductors*, Springer, Berlin, (2008).



- [15] G. W. Burr, B. N. Kurdi, J. C. Scott, C. H. Lam, K. Gopalakrishnan, R. S. Shenoy, Overview of candidate device technologies for storage-class memory, *IBM J. of Res. and Dev.*, (2008), 52 (4-5), pp. 449-464.
- [16] S. K. Halder, G. Sen, An X-ray determination of the thermal expansion of silver and copper-base alloys at high temperature. II. Cu-Ga, *Acta Cryst. A*, (1975), 31, pp. 158-159.